Mapping of putative binding sites on the ectodomain of the type II TGF-β receptor by scanning-deletion mutagenesis and knowledge-based modeling

Alain Guimond[1], Traian Sulea[1], Marie-Claude Pepin[2], Maureen D. O'Connor-McCourt*

Biotechnology Research Institute, National Research Council Canada, 6100 Royalmount Avenue, Montréal, Que. H4P 2R2, Canada

Received 4 June 1999

Abstract Binding surfaces of the type II transforming growth factor (TGF)-β receptor extracellular domain (TβRII-ECD) are mapped by combining scanning-deletion mutagenesis results with knowledge-based modeling of the ectodomain structure. Of the 17 deletion mutants produced within the core binding domain of TβRII-ECD, only three retained binding to TGF-β. Comparative modeling based on the crystal structure of the activin type II receptor extracellular domain (ActRII-ECD) indicates that the TβRII mutants which retain TGF-β binding are deleted in some of the loops connecting the β-strands in the TβRII-ECD model. Interpretation of the mutagenesis data within the structural framework of the ectodomain model allows for the prediction of potential binding sites at the surface of TβRII-ECD.

Key words: Type II transforming growth factor-β receptor; Scanning-deletion mutagenesis; Homology modeling

1. Introduction

Transforming growth factor-βs (TGF-βs) belong to a superfamily of factors that include activins, inhibins, the bone morphogenetic proteins and related morphogenetic peptides. Three closely related TGF-β isoforms (TGF-β1, -β2 and -β3) are found in mammals and these regulate many critical cellular processes such as cell growth, differentiation, extracellular matrix deposition and immune function [1,2]. The biological effects of TGF-βs are mediated by specific cell surface receptors which are present on almost all cell types [3]. Most cells have three types of TGF-β receptors designated as type I, type II and type III [4]. The type I [5] and type II [4] receptors are transmembrane serine/threonine kinases which have shown to be directly involved in signal transduction by forming a signaling complex in response to ligand binding [6]. The type I receptor is a 50–60 kDa protein that requires the presence of the type II receptor for TGF-β binding. In contrast, the type II receptor, a 75–85 kDa protein, can bind the ligand independently [6,7], but requires the presence of the type I receptor for signaling [6–8]. The type III receptor, also known as β-glycan, is a 200–300 kDa transmembrane proteoglycan which appears to 'present' TGF-β to the signaling receptors [9] by complexing with them in response to ligand. The enhancement of ligand binding by the type III receptor to the signaling receptors is particularly obvious for TGF-β2 since the signaling receptors alone have minimal affinity for this isoform. The absence of an obvious signaling motif in the cytoplasmic domain of the type III receptor, together with the fact that various TGF-β responsive cells lack the type III receptor [10,11], suggests that this receptor does not participate directly in TGF-β signal transduction. According to this model of TGF-β receptor signaling complex formation, the type II receptor can be considered as the primary sensor for the presence of TGF-β, the type I receptor as the effector and the type III receptor as an enhancer of the effective concentration of TGF-β. Although this overall scheme for the interaction of TGF-β with its receptors has been mapped out, very little is known about the structure of TGF-β receptor ectodomains. Only a few mutagenesis studies have been done to determine which subdomains and residues within the ectodomains are critical for ligand-receptor and receptor-receptor interactions.

With respect to the type III receptor, the original studies on mapping of the ligand binding site(s) within the ectodomain reported contradictory results. Two of the studies reported that a single binding site was located in the membrane proximal region of the ectodomain [12,13], while a third study localized a single binding site to the amino-terminal region [14]. More recent studies have suggested that the type III receptor contains two independent ligand binding sites [15,16]. However, it is not clear which of these is the predominant binding site [17,18]. No structural information is available on either of these ligand binding subdomains and detailed mutagenesis studies on the subdomains have not been reported.

In the case of the type I receptor, a three-dimensional (3D) model of the ectodomain has been constructed based on common sequence and structural features between the type I receptor and CD59 (protectin) [19]. The modeled structure contained four extending fingers and two clusters of charged residues. No mutagenesis studies have been reported on this ectodomain. Accordingly, it is not known which residues and structural determinants are important for the function.

With respect to the type II TGF-β receptor, one study, published by our group, reported a partial mapping of the extracellular ligand binding domain based on a scanning-deletion mutagenesis strategy [20]. In this analysis, a core binding domain for TGF-β was found to lie between amino acids 51 and 152 of the human type II TGF-β receptor extracellular domain (TβRII-ECD). However, no structural information is

*Corresponding author. Fax: (1) (514) 496-5143.
E-mail: maureen.o'connor@nrc.ca

[1] These authors contributed equally to this work.
[2] Present address: Les Laboratoires AEterna, 1405, boul. du Parc-Technologique, Ste-Foy, Que. G1P 4P5, Canada.

Abbreviations: ActRII-ECD, type II activin receptor extracellular domain; SCR, structurally conserved region; SVR, structurally variable region; TβRII-ECD, type II transforming growth factor-β receptor extracellular domain

0014-5793/99/$20.00
PII: S0014-5793(99)00869-8

presently available for the ectodomain of this receptor. More recently, the crystal structure of the extracellular domain of type II activin receptor (ActRII-ECD) has been experimentally resolved by X-ray crystallography [21]. It indicates that ActRII-ECD, and most likely the other family members including TβRII-ECD, adopt a fold similar to that of a class of toxins known as 'three-finger toxins'. In this paper, we extend this scanning-deletion mutagenesis to within the previously defined core binding domain of TβRII-ECD. We present a comparative structural model for TβRII-ECD based on the ActRII-ECD structure. The 3D model is used to rationalize the scanning-deletion mutagenesis results at the molecular level. Structural characteristics at the surface of the TβRII-ECD molecule which may play a role in ligand binding and specificity will also be discussed.

2. Materials and methods

2.1. Mutagenesis

Mutagenesis of the human TβRII subcloned in pCDNA-3 (Invitrogen) was done by the USE method as previously described [20,22]. Additional primers used in this analysis are as follows (numbers correspond to the deleted amino acids): Δ58-60: 5′-TTCTGGTTGTCACATCTCACATCACAAA, Δ63-65: 5′-TTGCTCATGCAGGAGTCACAGGTGGAAA, Δ68-70: 5′-GAGGTGATGCTGCAGCAGGATTTCTGGT, Δ73-75: 5′-GGCTTCTCACAGATGCTGCAGTTGCTCA, Δ78-80: 5′-ACACAGACTTCCTGACAGATGGAGGTGA, Δ83-85: 5′-TTTCTCCATACAGCTTCCTGTGGCTTCT, Δ88-90: 5′-ATGTTCTCGTCATTTACAGCCACACAGA, Δ93-95: 5′-ACTGTCTCTAGTGTGTCATTCTTTCTCC, Δ98-100: 5′-TTGGGGTCATGGCATAGTGTTATGTTCT, Δ103-105: 5′-TCATGGTAGGGGAGATGGCAAACTGTCT, Δ108-110: 5′-TCTTCCAGAATAAAGGGGAGCTTGGGGT, Δ113-115: 5′-TTTGGAGAAGCAGCAATAAAGTCATGGT, Δ118-120: 5′-TCCTTCATAATGCAAGCAGCATCTTCCA, Δ123-125: 5′-CCAGGCTTTTTTTTAATGCACTTTGGAG, Δ128-130: 5′-ATGAAGAAAGTCTCTTTTTTTTCCTTCA, Δ133-135: 5′-GAGCTACAGGAACAAGTCTCACCAGGCT, Δ143-145: 5′-GAGAAGATGATGTTCTCATCAGAGCTAC. The sequences of all mutants were confirmed by dideoxy sequencing (Pharmacia Biotech).

2.2. Cell culture, transfection and affinity labelling

293 cells were maintained in Dulbecco's modified Eagle medium supplemented with 10% fetal bovine serum (Hyclone). The day before transfection, the cells were seeded at 8×10^4 cells/well in a 12 well dish. The cells were transfected with 5 μl of Superfect reagent (Qiagen) and 1.5 μg of DNA according to the manufacturer's protocol. To monitor DNA uptake, 150 ng of GFPq plasmid (Quantum biotechnology) was included in each transfection. Following 3 h of incubation with Superfect reagent, the cells from each transfection were washed with phosphate-buffered saline, trypsinized and seeded in two equal aliquots. After 48 h at 37°C in 5% CO_2, half of the cells were affinity-labelled with [^{125}I]TGF-β1 as previously described [23]. The affinity-labelled receptors were solubilized and resolved on a reducing 4–12% gradient SDS-PAGE and exposed on a phosphorimager screen. The resulting image was displayed with Imagequant NT software (Molecular Dynamics). The remaining aliquot was use to measure GFPq DNA uptake by Flowcytometry on an EPICS XL-MCS (Beckman/Coulter).

2.3. Molecular modeling

The 3D model of residues 47–154 of TβRII-ECD was constructed by homology modeling using the program COMPOSER [24] implemented in SYBYL 6.4 software (Tripos, St. Louis, MO, USA). The X-ray-determined structure of ActRII-ECD, which adopts the three-finger toxin fold [21] (PDB code 1bte), was used as template. The target/template sequence alignment was adjusted manually to match the conserved disulfide pattern (Fig. 1b) as previously suggested [21]. Six structurally conserved regions (SCRs) were assigned in the initial

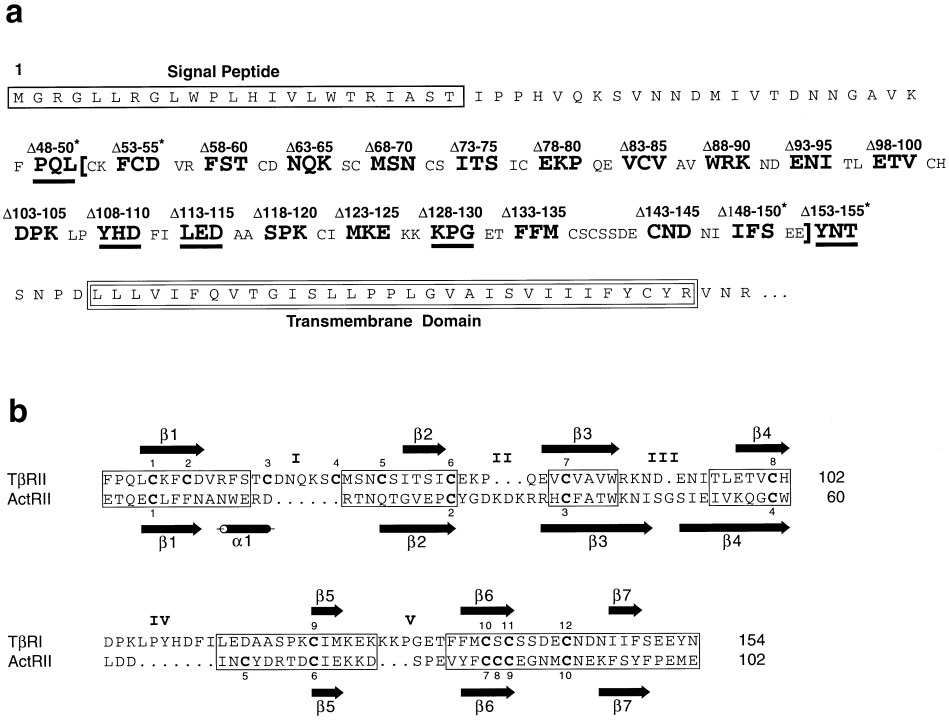

Fig. 1. (a) Schematic representation of the TβRII-ECD deletion mutants. Deleted amino acids are indicated in bold with the numbering such that amino acid number one is the first methionine. Mutants which bind [^{125}I]TGF-β1 are underlined. Brackets indicate the limits of the previously described core binding domain [20]. Mutants from that initial study are indicated by an asterisk. (b) Sequence alignment of the TβRII-ECD and ActRII-ECD used in homology modeling. SCRs are enclosed in boxes. Modeled SVRs are numbered I–V. Cysteine residues are bolded and numbered in their order of occurrence in the two sequences. Secondary structural elements as observed in the X-ray-determined structure of ActRII-ECD and in the modeled structure of TβRII-ECD are also shown and numbered in the order in which they appear in the sequence.

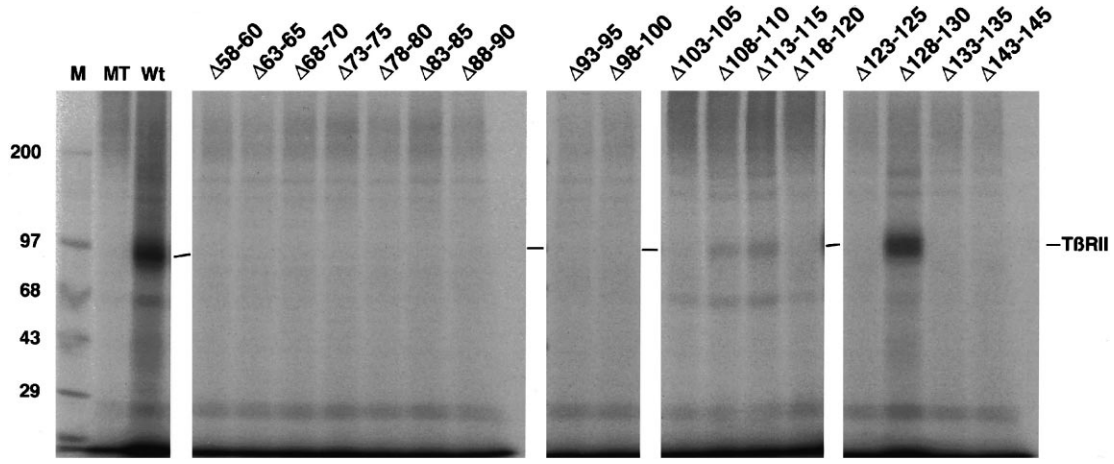

Fig. 2. Affinity labelling of 293 cells transiently transfected with TβRII deletion mutants. M: molecular weight markers (kDa), Wt: wild-type TβRII, MT: empty vector. Note: for some mutants (Wt, from Δ103-105 to Δ118-120), a band corresponding to the molecular weight of the type I TGF-β receptor is visible. This difference was not seen repeatedly and results from differences in the amount of endogenous type I receptor that is observed in different transfections.

model building. Five intervening structurally variable regions (SVRs I–V, i.e. loops with different length in TβRII-ECD and ActRII-ECD) were needed to complete a preliminary model structure (Fig. 1b). The conformations of SVRs II and III were copied from the corresponding loops with an identical length as cardiotoxin from *Naja nigricollis* (PDB code 1tgx) which adopts the same three-finger toxin fold [21,25]. The remaining SVRs were constructed by searching a database of protein structures deposited in PDB. In selecting loop conformations, the search output was examined for root mean square deviation in anchor positions, sequence homology as well as suitability to the overall tertiary structure. Model SVR I was obtained from hevamine A (PDB code 2hvm) and allowed proper formation of a disulfide bond. SVRs IV and V were modeled based on regions of lectin (PDB code 9wga) and core Gp32 DNA binding protein (PDB code 1gpc), respectively.

The disulfide pattern was assembled as C1-C7, C2-C5, C3-C4, C6-C8, C9-C10 and C11-C12 where the numbering of cysteine residues refers to their order of occurrence in the primary sequence of TβRII-ECD (Fig. 1b). Four of these disulfide bonds, C1-C7, C6-C8, C9-C10 and C11-12, correspond to C1-C3, C2-C4, C6-C7 and C9-C10 disulfides, respectively, found in the ActRII-ECD template structure [21]. In the initial model building of the SCRs, Cys-54 and Cys-71 were positioned proximally enough to allow pairing (C2-C5 disulfide) of two out of the four additional cysteines in the N-terminal segment of TβRII-ECD. The remaining disulfide C3-C4 was provided by database search in SVR I. N- and C-termini were blocked with acetyl- and methylamino groups, respectively, and hydrogen atoms were added explicitly using the BIOPOLYMER module of SYBYL 6.4. Structural refinement was performed in SYBYL 6.4 by energy minimization using AMBER 4.1 all-atom force-field [26] with the Powel minimizer, a distance-dependent (4r) dielectric constant and an 8 Å non-bonded cut-off. Preliminary stages of energy minimization were performed (i) in the SVRs only, followed by (ii) fixing the position of SCRs backbone atoms only. All the constraints were then released and the energy minimization was carried out until the root mean square of the gradients was smaller than 0.01 kcal/mol Å.

3. Results and discussion

In our previous scanning-deletion mutagenesis study, three amino acid deletions were introduced at intervals of five amino acids within the N-terminal and C-terminal ends of the extracellular domain of TβRII. The resulting constructs were analyzed by affinity labelling of transfected Cos-1 cells [20]. A core domain for TGF-β binding was mapped from residues 51 to 152. We have now extended this analysis to within the core domain itself by producing 17 additional deletion mutants (Fig. 1a). Each mutant construct was evaluated for ligand binding by transient transfection in 293 cells. Following a 48 h period of expression, the cells were cross-link-labelled with iodinated TGF-β1 and cell extracts were analyzed by SDS-PAGE and phosphorimaging. Among the 17 new mutants, only three (Δ108-110, Δ113-115 and Δ128-130) were found to be affinity-labelled with [^{125}I]TGF-β at a detectable level. The amount of affinity labelling for mutants Δ108-110 and Δ113-115 is lower than that of mutant Δ128-130, which is not significantly different from that of the wild-type TβRII (Fig. 2).

The scanning-deletion mutagenesis results were translated into the 3D structural context provided by a homology model of the TβRII-ECD which is based on the recently determined structure of ActRII-ECD [21]. The overall structure of the TβRII-ECD model adopts the three-finger toxin fold comprising seven β-strands which form three anti-parallel sheets (Fig. 3a). It also contains six disulfide bonds (see Section 2), four of which are formed by eight cysteines which are characteristic of the three-finger toxin fold and conserved in ActRII-ECD [21]. The fold is further stabilized by two significant hydrophobic clusters, one partly buried between strands β3, β6 and β7 and the other one largely exposed at the bottom of the cavity formed on the concave side of the extracellular domain. Substantial insertions relative to the ActRII-ECD (totaling 16 residues) occurred in the β1-β2 (finger 1), β4-β5 and β5-β6 (finger 3) loop regions (Fig. 1b) and result in a more pronounced curvature of the convex and concave faces of the TβRII-ECD molecule (Fig. 3b and c) as compared to the ActRII-ECD template [21].

Model building of the TβRII-ECD structure allows us to rationalize the experimental results by projecting the three residue deletions onto the secondary structural elements and molecular surface of the ectodomain (Fig. 3). The present scanning-deletion analysis indicates that three TβRII-ECD deletion mutants (Δ108-110, Δ113-115 and Δ128-130) are able to bind TGF-β. This demonstrates not only that all these mutants are both properly folded and readily expressed at the cell surface, but more importantly that they preserve all structural determinants required for interaction with the ligand. According to our model, these three deletions are located in

rather peripheral regions within loops connecting the β-strands (Fig. 3a). In general, deletions in such regions are likely to induce more localized effects, rather than profound structural alterations of the domain. Two of the mutants that bind TGF-β (Δ108-110 and Δ113-115) are deleted in the loop connecting β4- and β5-strands (Fig. 3a). It is in this loop that an insertion in TβRII-ECD versus ActRII-ECD occurs (Fig. 1b). The third binding mutant (Δ128-130) lacks three residues in the finger 3 loop of TβRII-ECD (Fig. 3a). Once again, this is a loop where there is an insertion relative to the template ActRII-ECD structure (Fig. 1b). We also show in our model the deletion mutants Δ48-50 and Δ153-155 (Fig. 1a) which, we previously demonstrated, did not alter binding [20]. Spatial distribution of these five deletions allows for the identification of two areas on the TβRII-ECD that are not important for ligand binding (Fig. 3). They are located in the vicinity of (i) residues 48–50, 108–110 and 113–115 close to the N-terminus and (ii) residues 128–130 and 153–155 close to the C-terminus of the domain.

Since the scanning-deletion technique is more structurally disruptive than scanning-point mutagenesis, the functional interpretation of the three residue deletions which lead to inactive TβRII mutants is complicated by the fact that a lack of binding may be due to major conformational changes in the domain as a whole (i.e. unfolding or misfolding), at least for some of the mutants. The homology model offers an approach to rationally interpret these non-binding mutants. Eight of the mutants have deletions which fall, partially or completely, within the β-sheet system (and implicitly within the hydrophobic clusters) which occupies a central position within the domain structure (Fig. 3a): Δ53-55, Δ73-75, Δ83-85, Δ88-90, Δ98-100, Δ123-125, Δ133-135 and Δ148-150. In addition, the Δ143-145 deletion removes residues Cys-143 and Asn-144 (conserved in all type II receptors) thus precluding C11-C12 disulfide bond formation and H-bond anchoring of β1- and β3-strands, respectively. It is therefore not surprising that all the mutants containing these deletions do not bind TGF-β, an effect that is suspected to arise from significant structural changes in the receptor. However, the observed lack of binding might be attributed in part, at least for some of these mutants, to the removal of important interactive binding sites as suggested by an analysis of the surface properties of the modeled domain molecule (see below).

The remaining seven mutants that do not bind TGF-β have deletions in the loops connecting the β-strands of the domain (Fig. 3a). The three deletions engineered in the finger 1 loop region (Δ58-60, Δ63-65 and Δ68-70) are unlikely to induce major conformational rearrangements within the ectodomain, since both ActRII-ECD and cardiotoxin display a much shorter finger 1 without affecting the H-bond interactions between β1- and β2-strands [21,25]. Instead, it is likely that these deletions cause only local perturbations, supporting the concept that the highly variable finger 1 may be important for specific binding interactions [21]. The presence of two disulfide bonds in finger 1 (C2-C5 which sets the loop anchor positions and C3-C4 which provides additional constraint within the loop itself) may be required for stabilizing the bioactive conformation of this loop. Some of the deletions in the finger 1 region may eliminate residues that are required for direct contact with the TGF-β, whereas other deletions in this loop may abolish binding indirectly by rendering the local loop conformation inactive. Residues 78–80 in the loop connecting the β2- and β3-strands may also play a role in ligand binding. Although three residues longer, the corresponding loop in ActRII-ECD is distorted in one of the two molecules in the asymmetric unit and therefore, it has been speculated that this loop may play a role in receptor recognition [21]. The elimination of residues 93–95 in the loop connecting the β3- and β4-strands (finger 2) also resulted in an inactive variant of the receptor. However, the somewhat extended conformation of

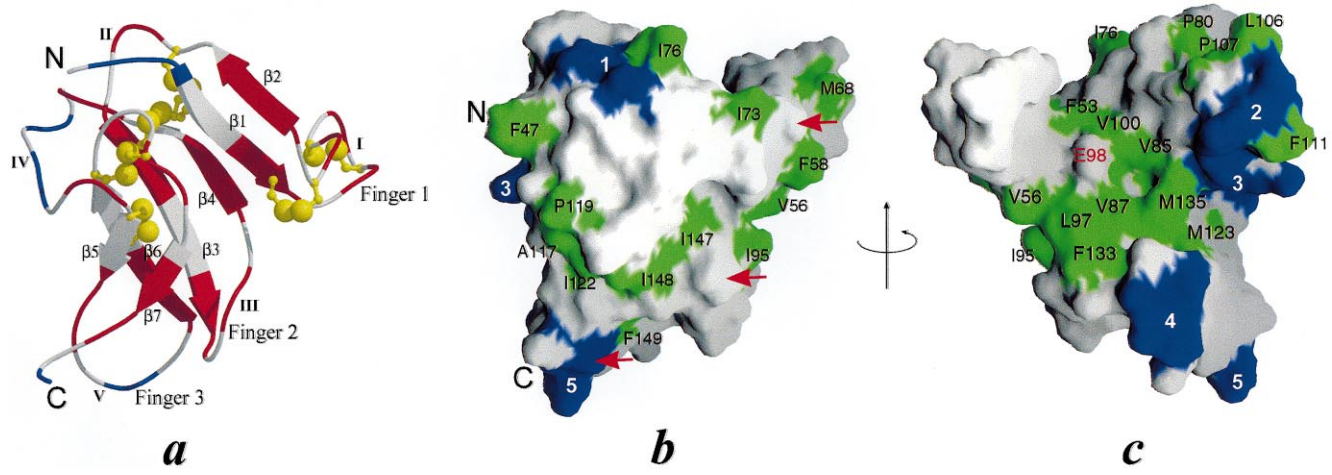

Fig. 3. Mapping of the scanning-deletion mutagenesis results onto the homology model of TβRII-ECD. (a) Ribbon representation of the TβRII-ECD model structure. Three residue deletions are colored in red for the mutants that do not bind TGF-β and in blue for those that bind TGF-β. Side-chains of cysteine residues are colored in yellow and shown as ball and stick with the sulfur atom represented as CPK. Strands are numbered in the order in which they occur in the sequence. The modeled SVRs numbered I–V in Fig. 1b are also labelled. (b) Molecular surface representation of the TβRII-ECD model structure displayed with the convex side in front in an orientation similar to that shown in a and (c) with the concave side in front corresponding to a ~180° rotation relative to the orientation in a and b. Surface areas corresponding to the five deletions that lead to active mutants are colored in blue and identified as 1 for Δ48-50, 2 for Δ108-110, 3 for Δ113-115, 4 for Δ128-130 and 5 for Δ153-154. The molecular surface associated with the side-chain atoms of hydrophobic residues Ala, Ile, Leu, Met, Phe, Pro and Val is colored in green and labelled by a residue number (there is only one Trp residue which is completely buried and only one Tyr which belongs to surface area 3). Residue Glu-98 is labelled in red. Putative glycosylation sites (Asn-70, Asn-94 and Asn-154) are marked with red arrows.

this loop suggests that the lack of binding properties may be due to global structural changes in the ectodomain rather than removal of an important interacting site. The inactivity of two of the mutants with deletions in the loop linking β4- and β5-strands (Δ103-105 and Δ118-120) is likely to be more directly related to the removal of specific interacting residues of the ectodomain rather than to global or local loop conformational rearrangement. We conclude this since the adjacent deletions (Δ108-110, Δ113-115) in the loop did not abolish binding, even though the conformation of the loop would be affected.

The results of the scanning-deletion mutagenesis combined with the knowledge-based modeling have enabled us to delineate potential sites on the surface of the TβRII-ECD that are required for the binding of TGF-β. In general, exposed hydrophobic patches on a protein surface tend to be part of a binding interface [27,28]. In order to assess and prioritize the potential binding sites further, we mapped the position of solvent-exposed clustered hydrophobic side-chains on the surface of TβRII-ECD. It can be seen that none of the mutants that retain activity has deletions which interfere with surface hydrophobic regions (Fig. 3b and c). By far, the most significant potential protein binding interface is formed by the solvent-exposed hydrophobic patch lining the bottom of the cavity on the concave face of the molecule (Fig. 3c). The residues contributing to the patch arise from the central β-strands of the domain: Phe-53 from β1, Val-85 and Val-87 from β3, Leu-97 and Val-100 from β4, Met-123 from β5, Phe-133 and Met-135 from β6. Some of these residues were eliminated during the scanning-deletion analysis in mutants which do not bind TGF-β (Δ53-55, Δ83-85, Δ98-100, Δ123-125, Δ133-135), further supporting the presence of a binding interface in this region. However, as we discussed earlier, it is difficult to attribute the inactivity of these mutants to only one of the two 'concomitant' changes that likely occur upon deletion: the alteration of the binding site integrity and the modification of folding properties of the ectodomain. A similar hydrophobic patch has been identified in the ActRII-ECD structure [21]. Multiple conservative mutations in the corresponding hydrophobic side-chains, complemented by differences in more localized features (e.g. the position of a small pocket and an adjacent charge reversal, Glu-98 in TβRII-ECD versus Lys-56 in ActRII-ECD, in the center of the patch), may play an important role in determining the specificity of these type II receptors for their natural ligands. The second significant hydrophobic patch is located on the convex face of the molecule (Fig. 3b). There exists a corresponding patch in ActRII-ECD as well [21]. The contributing residues belong to strands β5 (Ile-122), β7 (Ile-147 and Ile-148) and the C-terminal part of the loop connecting β4 and β5 (Ala-117 and Pro-119). The importance of this patch is supported by the lack of TGF-β binding to the deletion mutants Δ118-120 and Δ148-150 in which residues Pro-119 and Ile-148, respectively, are not present. It is worth stressing that all the residues forming these two potential binding sites belong to SCRs, which are characterized by higher model accuracy in comparison with modeled SVRs. In addition to these two major patches, there are two much less extended hydrophobic surface areas that may be required for interactions. One of them, which flanks one side of the concave face of the domain, is formed by residues from the loop connecting β2- and β3-strands (Pro-80 was removed in the inactive mutant Δ78-80) and the N-terminal segment of the loop between β4 and β5 (Leu-106 and Pro-107). The other one is located at the interface between fingers 1 and 2 and formed by side-chains of Phe-58 and Ile-95 (residues deleted in the inactive mutants Δ58-60 and Δ93-95, respectively) as well as the Cys-54-Cys-71 disulfide (disrupted in the inactive mutant Δ53-55).

The interpretation above can be complemented by the reported data on the effect of *N*-glycosylation on the binding properties of TβRII. It has been shown that the glycosylation of either TβRII or ActRII does not significantly affect ligand binding [29,30] and therefore, these glycosylation sites should not fall within the binding interface(s). There are three possible *N*-glycosylation sites within the TβRII-ECD (Asn-70, Asn-94 and Asn-154). For ActRII-ECD, the glycosylation of Asn-24, which corresponds to Asn-70 in TβRII-ECD, has been demonstrated by X-ray crystallography [21]. The structural model of the TβRII-ECD shows that these three glycosylation sites are accessible to the solvent (Fig. 3b). During the scanning-deletion mutagenesis study, all the putative glycosylation sites have been removed (Asn-70 in the Δ68-70 mutant, Asn-94 in the Δ93-95 mutant and Asn-154 in the Δ153-155 mutant). The fact that the deletion of the Asn-70 glycosylation site in Δ68-70 causes a loss of binding supports the concept that residues 68–70 are important in stabilizing a particular bioactive conformation of the finger 1 loop rather than directly interacting with TGF-β. The predicted binding region of finger 1 is therefore likely positioned on the side of the loop which is opposite to residues 68–70 facing the concave face of the domain and corresponding to the residues deleted in the inactive mutants Δ58-60 and Δ63-65. The inactivity of the mutant with the putative glycosylation site Asn-94 excised (Δ93-95) suggests a structural rather than interacting role for residues 93–95, as discussed earlier. Finally, the elimination of the third possible glycosylation site, Asn-154 in Δ153-155, does not alter the binding capability of this mutant. This further supports the location of this stretch of residues as being further away from the binding sites of the domain.

The combination of scanning-deletion mutagenesis with structural model building is a powerful technique that has allowed us to rationally identify putative binding sites on the TβRII-ECD. Our results represent the first attempt to map a functional profile onto the structural features of the TβRII-ECD. There are, however, inherent limitations in our knowledge-based model of the domain, in particular in the loop regions. A more precise structure of the domain has to be determined via experimental studies (e.g. X-ray or NMR). Further biochemical and docking experiments are currently underway in order to more accurately map the binding interface of the of type II TGF-β receptor extracellular domain with its natural partner molecules.

Acknowledgements: The authors wish to thank Dr Michel Beauchemin for his participation in the early stages of this work. NRCC publication 42920.

References

[1] Roberts, A.B. and Sporn, M.B. (1990) in: Handbook of Experimental Pharmacology. Peptide Growth Factors and Their Receptors (Sporn, M.B. and Roberts, A.B., Eds.), pp. 419–472, Springer-Verlag, New York.
[2] Roberts, A.B. and Sporn, M.B. (1993) Growth Factors 8, 1–9.

[3] Wakefield, L.M., Smith, D.M., Masui, T., Harris, C.C. and Sporn, M.B. (1987) J. Cell. Biol. 105, 965–975.
[4] Lin, H.Y., Wang, X.-F., Ng-Eaton, E., Wainberg, R.A. and Lodish, H.F. (1992) Cell 68, 775–785.
[5] Franzen, P., ten Dijke, P., Ichijo, H., Yamashita, H., Schulz, P., Heldin, C.H. and Miyazono, K. (1993) Cell 75, 681–692.
[6] Wrana, J.L., Attisano, L., Càrcamo, J., Zentella, A., Doodey, J., Laiho, M., Wang, X.-F. and Massagué, J. (1992) Cell 71, 1003–1014.
[7] Laiho, M., Weis, M.B. and Massagué, J. (1990) J. Biol. Chem. 265, 18518–18524.
[8] Laiho, M., Weis, M.B. and Massagué, J. (1991) J. Biol. Chem. 266, 9108–9112.
[9] López-Casillas, F., Wrana, J.L. and Massagué, J. (1993) Cell 73, 1435–1444.
[10] Segarini, P.R., Rosen, D.M. and Seyedin, S.M. (1989) Mol. Endocrinol. 3, 261–272.
[11] Cheifetz, S., Hernandez, H., Laiho, M., ten Dijke, P., Iwata, K.K. and Massagué, J. (1990) J. Biol. Chem. 265, 20533–20538.
[12] Pepin, M.C., Beauchemin, M., Plamondon, J. and O'Connor-McCourt, M.D. (1994) Proc. Natl. Acad. Sci. USA 91, 6997–7001.
[13] Fukushima, D., Bützow, R., Hildebrand, A. and Ruoslahti, E. (1993) J. Biol. Chem. 268, 22710–22715.
[14] López-Casillas, F., Payne, H.M., Andres, J.L. and Massagué, J. (1994) J. Cell Biol. 124, 557–568.
[15] Pepin, M.C., Beauchemin, M., Collins, C., Plamondon, J. and O'Connor-McCourt, M.D. (1995) FEBS Lett. 377, 368–372.
[16] Matsuzaki, K., Kan, M. and Mckeehan, W.L. (1996) In Vitro Cell Dev. Biol. Anim. 32, 345–360.
[17] Taniguchi, A., Matsuzaki, K., Nakano, K., Kan, M. and Mckeehan, W.L. (1998) In Vitro Cell Dev. Biol. Anim. 34, 232–238.
[18] Philip, A., Hannah, R. and O'Connor-McCourt, M. (1999) Eur. J. Biochem. 261, 618–628.
[19] Jokiranta, T.S., Tissari, J., Teleman, O. and Meri, S. (1995) FEBS Lett. 376, 31–36.
[20] Pepin, M.C., Beauchemin, M., Plamondon, J. and O'Connor-McCourt, M.D. (1996) Biochem. Biophys. Res. Commun. 220, 289–293.
[21] Greenwald, J., Fischer, W.H., Vale, W.W. and Choe, S. (1999) Nat. Struct. Biol. 6, 18–22.
[22] Deng, W.P. and Nickoloff, J.A. (1992) Anal. Biochem. 200, 81–88.
[23] Philip, A. and O'Connor-McCourt, M.D. (1991) J. Biol. Chem. 266, 22290–22296.
[24] Sutcliffe, M.J., Haneef, I., Carney, D. and Blundell, T.L. (1987) Protein Eng. 1, 377–384.
[25] Bilwes, A., Rees, B., Moras, D., Menez, R. and Menez, A. (1994) J. Mol. Biol. 239, 122–136.
[26] Cornell, W.D., Cieplak, P., Bayly, C.I., Gould, I.R., Merz Jr., K.M., Ferguson, D.M., Spellmeyer, D.C., Fox, T., Caldwell, J.W. and Kollman, P.A. (1995) J. Am. Chem. Soc. 177, 5179–5197.
[27] Young, L., Jernigan, R.L. and Covell, D.G. (1994) Protein Sci. 3, 717–729.
[28] Clackson, T. and Wells, J.A. (1995) Science 267, 383–386.
[29] Lin, H.Y., Moustakas, A., Knaus, P., Wells, R.G., Henis, Y.I. and Lodish, H.F. (1995) J. Biol. Chem. 270, 2747–2754.
[30] Greenwald, J., Le, V., Corrigan, A., Fischer, W., Komives, E., Vale, W. and Choe, S. (1998) Biochemistry 37, 16711–16718.